Field-induced multiple-point quantum criticality in the three-leg Heisenberg ladder

Mohamed Azzouz
Department of Physics, Laurentian University, Ramsey Lake Road, Sudbury, Ontario, Canada P3E 2C6
and School of Science and Engineering, Al Akhawayn University, Avenue Hassan II, Ifrane 53000, Morocco
(Received 31 October 2007; published 22 July 2008)

Field-induced quantum (zero temperature) criticality described using parameters that are not associated with a symmetry-breaking long-range order is found in the spin-$\frac{1}{2}$ antiferromagnetic three-leg Heisenberg ladder. These parameters represent the spin bond order, which is a consequence of the probability for spins on adjacent sites to be bound in a singletlike arrangement. They underwent two phase transitions, one at the lower critical field h_{c1} and the other at the upper critical field h_{c2}. The field dependence of these bond parameters and of the magnetization is calculated for several values of the rung coupling in all regimes. This yields the coupling field phase diagram. It is found that the rung coupling must exceed a threshold value for the plateau, at one third of the saturation magnetization, to appear. The results obtained here within the bond mean-field theory compare well with existing numerical data.

DOI: 10.1103/PhysRevB.78.014421 PACS number(s): 75.10.Jm, 73.43.Nq, 75.10.Pq, 75.10.Dg

I. INTRODUCTION

Quantum or zero-temperature criticality has attracted a significant attention in strongly correlated electron systems.[1] Recently, field-induced quantum criticality has been found in the spin-$\frac{1}{2}$ Heisenberg chain and two-leg ladder.[2] In the chain, the spin bond parameter[3] undergoes a zero-temperature phase transition at the same magnetic field where the magnetization saturates. The three-leg ladder is known to renormalize down to a single chain in the low-energy limit.[4] Because its energy spectra[5] consist of more than one band contrary to the chain, one expects a richer coupling field phase diagram, which we calculate here for the three-leg ladder. We recover the fact that in the strong rung coupling limit, the three-leg ladder has a magnetization versus magnetic field characterized by a plateau at one third of the saturation value M_s and by a saturation plateau in the strong-field limit.[6–8] In addition, we show that this system is characterized by spin bond parameters that display zero-temperature criticality and plateaus too. It is also found that the rung coupling must exceed a threshold value for the plateau at one third of saturation to occur in the magnetization and in the bond parameters. The mechanism responsible for these plateaus and criticality is explained using the energy spectra of the Jordan-Wigner[3,9] (JW) fermions that are used to map the spin-$\frac{1}{2}$ degrees of freedom.

The density-matrix renormalization group (DMRG) technique and the strong-coupling series expansion have been used successfully to study the antiferromagnetic (AF) Heisenberg model on the three-leg ladder in the strong-coupling regime.[6–8] However, in the intermediate-coupling and weak-coupling regimes, the strong-coupling series expansion obviously breaks down and the DMRG utilized by Tandon *et al.*[6] used the existence of a magnetization plateau as a prerequisite. As we find here, there is no plateau at the third of the saturation magnetization in the weak rung coupling regime. Moreover, the bosonization technique becomes doubtful when the rung coupling exceeds a value of the order of the chain coupling. This therefore justifies the need for a method, such as the one applied here, valid in all coupling regimes.

This paper is organized as follows: In Sec. II, we analyze the AF three-leg ladder in a uniform magnetic field using the bond mean-field theory[3] (BMFT). In Sec. III we study the field dependence of zero-temperature magnetization and susceptibility. Section IV deals with the field dependence of the bond mean-field parameters. Section V explains for the mechanism that causes the plateaus in both magnetization and spin bond parameters. In Sec. VI, the effect of temperature on the field dependence of magnetization, susceptibility, and spin bond parameters is worked out. In Sec. VII, an analytical solution that shows the occurrence of the quantum phase transitions in the three-leg ladder is presented. In Sec. VIII conclusions are drawn.

II. THREE-LEG HEISENBERG LADDER IN A MAGNETIC FIELD

A. Derivation of the BMFT energy spectra

We extend the BMFT used in Refs. 2 and 5 to the case where an external magnetic field is applied to the three-leg ladder. The AF Heisenberg model on this system (Fig. 1) is given by the following Hamiltonian:

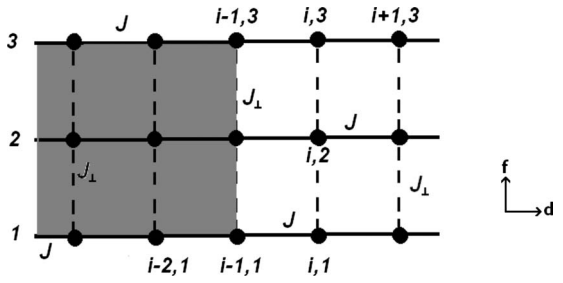

FIG. 1. Sites within the shaded area are taken into account in the calculation of the phase $\Phi_{i,1}$ of $S_{i,1}$ in the JW transformation [Eq. (2)] for the three-leg ladder. The phase for sites $S_{i,2}$ and $S_{i,3}$ are obtained by adding to $\Phi_{i,1}$, $\pi n_{i,1}$, and $\pi(n_{i,1}+n_{i,2})$, respectively.

$$H = \sum_{i=1}^{N} \left(\sum_{j=1}^{3} J \mathbf{S}_{i,j} \mathbf{S}_{i+1,j} + \sum_{j=1}^{2} J_{\perp} \mathbf{S}_{i,j} \cdot \mathbf{S}_{i,j+1} \right) - g \mu_B B \sum_{i,j} S_{i,j}^{z}, \tag{1}$$

where $J>0$ and $J_{\perp}>0$ are the exchange coupling constants along the chains and rungs, respectively. The index $i=0, \ldots, N-1$ labels the N sites on each of the chains and $j=1,2,3$ labels the chains. We define $\alpha=J_{\perp}/J$ and set J to be the unit of energy. B designates the applied magnetic field, g designates the Landé factor, and μ_B designates the Bohr magneton. For simplicity we define $h=g\mu_B B$. The open boundary conditions (BCs) along the rungs and the periodic boundary ones along the chains are considered.

The Hamiltonian Eq. (1) is transformed using the two-dimensional (2D) generalized JW transformation of Ref. 3, which is adapted to the three-leg ladder geometry. Following the notation of Fig. 1, the spin operators at sites $(i,1)$, $(i,2)$, and $(i,3)$ are written as follows:

$$S_{i,1}^{-} = c_{i,1} e^{i\Phi_{i,1}}, \quad \Phi_{i,1} = \pi \sum_{d=0}^{i-1} \sum_{f=1}^{3} n_{d,f},$$

$$S_{i,2}^{-} = c_{i,2} e^{i\Phi_{i,2}}, \quad \Phi_{i,2} = \Phi_{i,1} + \pi n_{i,1},$$

$$S_{i,3}^{-} = c_{i,3} e^{i\Phi_{i,3}}, \quad \Phi_{i,3} = \Phi_{i,2} + \pi n_{i,2},$$

$$S_{i,j}^{z} = c_{i,j}^{\dagger} c_{i,j} - \frac{1}{2}, \tag{2}$$

where $n_{i,j}=c_{i,j}^{\dagger}c_{i,j}$ is the occupation operator for the JW fermions. The BMFT consists on one hand by approximating the sum of the phase differences resulting to the hopping of the JW fermions around each plaquette by π.[2,3,10] When written, using the JW transformation, the quartic Ising terms of Hamiltonian Eq. (1) yield on the other hand terms of the form,

$$\sum_{i,j} (J n_{i,j} n_{i+1,j} + J_{\perp} n_{i,j} n_{i,j+1}), \tag{3}$$

which are decoupled using the bond parameters $Q=\langle c_{2i,j} c_{2i+1,j}^{\dagger} \rangle$ for chain one $(j=1)$ and chain three $(j=3)$, and $Q'=\langle c_{2i,2} c_{2i+1,2}^{\dagger} \rangle$ for chain two in the direction parallel to the chains. $P=\langle c_{i,j} c_{i,j+1}^{\dagger} \rangle$ is used to decouple the interactions along the rungs. This choice is consistent with the fact that the three-leg ladder is symmetric with respect to exchanging the chain labels one and three.[5] The parameters Q, Q', and P can be interpreted as the probability for the spins on any two adjacent sites to be found in a singlet arrangement because $\langle c_{\mathbf{r}} c_{\mathbf{r}'}^{\dagger} \rangle \sim \langle S_{\mathbf{r}}^{-} S_{\mathbf{r}'}^{+} \rangle$. $\mathbf{r}$ and $\mathbf{r}'$ designate two adjacent sites. When these parameters are nonzero, it becomes possible for all spins to pair in order to form such singlets, thus giving some kind of ordering that does not break symmetry.

Exact numerical methods show that the magnetization in the three-leg Heisenberg ladder (with open BCs along the rungs) increases linearly with external magnetic field.[6] This is a consequence of the fact that in zero field and temperature this system behaves as a single chain with a renormalized coupling in the strong rung coupling.[5] For the Heisenberg chain, it is known that the magnetization increases linearly with field in the weak-field regime.[11] Thus, we have to consider as well the decoupling of the Ising term using the parameter $\langle c_{i,j}^{\dagger} c_{i,j} \rangle$ that is related to the uniform magnetization $M_z=\langle S_i^z \rangle$ by

$$\langle c_{i,j}^{\dagger} c_{i,j} \rangle = M_z + 1/2, \tag{4}$$

as a result of Eq. (2). Thus considering this magnetization channel in the decoupling procedure, one gets

$$S_{i,j}^{z} S_{i',j'}^{z} \approx M_z S_{i,j}^{z} + M_z S_{i',j'}^{z} - M_z^2$$
$$= M_z n_{i,j} + M_z n_{i',j'} - M_z(M_z+1). \tag{5}$$

Further details on the BMFT can be found elsewhere.[12–15] Fourier transforming along the chains (while keeping the chain labels in the real space) and using the Nambu formalism[16] on a bipartite lattice (with sublattices A and B) yield the following mean-field Hamiltonian:

$$H = \sum_{k} \Psi_k^{\dagger} \mathcal{H} \Psi_k - N(3J + 2J_{\perp}) M_z(M_z+1)$$
$$+ N\left(2JQ^2 + JQ'^2 + 2J_{\perp}P^2 + \frac{3}{2}h \right), \tag{6}$$

where the Nambu spinor is given by

$$\Psi_k^{\dagger} = (c_{1k}^{A\dagger} c_{1k}^{B\dagger} c_{2k}^{A\dagger} c_{2k}^{B\dagger} c_{3k}^{A\dagger} c_{3k}^{B\dagger}), \tag{7}$$

and the Hamiltonian density by

$$\mathcal{H} = \begin{bmatrix} -h' & e(k) & 0 & \frac{J_{\perp 1}}{2} & 0 & 0 \\ e^*(k) & -h' & \frac{J_{\perp 1}}{2} & 0 & 0 & 0 \\ 0 & \frac{J_{\perp 1}}{2} & -h'' & e'(k) & 0 & \frac{J_{\perp 1}}{2} \\ \frac{J_{\perp 1}}{2} & 0 & e'^*(k) & -h'' & \frac{J_{\perp 1}}{2} & 0 \\ 0 & 0 & 0 & \frac{J_{\perp 1}}{2} & -h' & e(k) \\ 0 & 0 & \frac{J_{\perp 1}}{2} & 0 & e^*(k) & -h' \end{bmatrix}, \tag{8}$$

with $e(k)=iJ_1 \sin k$, $e'(k)=iJ_1' \sin k$, $h'=h-(2J+J_{\perp})M_z$, and $h''=h-2(J+J_{\perp})M_z$. Notice the difference in the $J_{\perp}$ dependence in h' and h''. The factor two in $2J_{\perp}$ in h'' is a result of the fact that each of the spins on sites belonging to the internal chain is coupled to two spins; each on one of the outer chains. This is not the case for each of the spins on the outer chains, which are coupled to a single spin only along the rungs. Diagonalizing $\mathcal{H}$ yields the following eigenenergies:

$$E_1^{\pm}(k) = -h' \pm J_1 \sin k,$$

$$E_2^{\pm}(k) = \frac{1}{2}[(J_1 - J_1')\sin k - h' - h'' \pm \epsilon_{-}(k)],$$

$$E_3^{\pm}(k) = \frac{1}{2}[(J_1' - J_1)\sin k - h' - h'' \pm \epsilon_+(k)], \tag{9}$$

with

$$\epsilon_{\pm}(k) = \sqrt{[(J_1 + J_1')\sin k \pm J_\perp M_z]^2 + 2J_{\perp 1}^2},$$

$$J_1 = J(1+2Q),$$

$$J_1' = J(1+2Q'),$$

$$J_{\perp 1} = J_\perp(1+2P). \tag{10}$$

In zero external fields, the three-leg ladder has been studied using the same method as here. The energy excitation spectrum $E_1(k)$ with $h=0$ has the same form as the des Cloizeaux–Pearson spectrum of the AF Heisenberg chain.[17] $E_2(k)$ and $E_3(k)$ are characterized by a gap of the order of $J_\perp$. Thus, in the case of zero applied field the energy excitations consist of three bands, two of which are gapped.[5]

Next, we will derive the mean-field equations satisfied by the bond parameters in the cases $Q \neq Q'$ and $Q' = Q$. We will calculate the field dependence for both cases and find out which state is the stable one thermodynamically.

B. Mean-field equations for the state with $Q \neq Q'$: State I

In the present mean-field approach, the free energy per site corresponding to Hamiltonian Eq. (6) is

$$f_{\mathrm{I}}(T,h) = \frac{1}{3}(2JQ^2 + JQ'^2 + 2J_\perp P^2) - \frac{1}{3}(3J + 2J_\perp)M_z(M_z+1) + \frac{h}{2} - \frac{k_B T}{2N_t}\sum_k \sum_{s=\pm} \sum_{j=1}^{3} \ln[1 + e^{-\beta E_j^s(k)}], \tag{11}$$

where $N_t = 3N$ is the total number of lattice sites and $\beta = 1/k_B T$, with k_B being Boltzmann constant. The parameters Q, Q', and P are determined by minimizing $f_{\mathrm{I}}(T,h)$ with respect to all three bond parameters; $\partial f_{\mathrm{I}}/\partial Q = \partial f_{\mathrm{I}}/\partial Q' = \partial f_{\mathrm{I}}/\partial P = 0$. This gives

$$Q = \frac{-1}{8JN}\sum_k \sum_{s=\pm} \sum_{j=1}^{3} \frac{\partial E_j^s(k)}{\partial Q} n_F[E_j^s(k)],$$

$$Q' = \frac{-1}{4JN}\sum_k \sum_{s=\pm} \sum_{j=2}^{3} \frac{\partial E_j^s(k)}{\partial Q'} n_F[E_j^s(k)],$$

$$P = \frac{-1}{8J_\perp N}\sum_k \sum_{s=\pm} \sum_{j=2}^{3} \frac{\partial E_j^s(k)}{\partial P} n_F[E_j^s(k)], \tag{12}$$

with

$$\frac{\partial E_1^s}{\partial Q} = 2sJ \sin k,$$

$$\frac{\partial E_2^s}{\partial Q} = J \sin k \left\{ 1 + \frac{s[(J_1 + J_1')\sin k - J_\perp M_z]}{\epsilon_-(k)} \right\},$$

$$\frac{\partial E_3^s}{\partial Q} = J \sin k \left\{ -1 + \frac{s[(J_1 + J_1')\sin k + J_\perp M_z]}{\epsilon_+(k)} \right\},$$

$$\frac{\partial E_2^s}{\partial Q'} = J \sin k \left\{ -1 + \frac{s[(J_1 + J_1')\sin k - J_\perp M_z]}{\epsilon_-(k)} \right\},$$

$$\frac{\partial E_3^s}{\partial Q'} = J \sin k \left\{ 1 + \frac{s[(J_1 + J_1')\sin k + J_\perp M_z]}{\epsilon_+(k)} \right\},$$

$$\frac{\partial E_2^s}{\partial P} = \frac{2sJ_\perp J_{\perp 1}}{\epsilon_-(k)},$$

$$\frac{\partial E_3^s}{\partial P} = \frac{2sJ_\perp J_{\perp 1}}{\epsilon_+(k)}, \quad s = \pm. \tag{13}$$

The magnetization $M_z = -\partial f_{\mathrm{I}}/\partial h$ is given by

$$M_z = \frac{1}{6N}\sum_k \sum_{s=\pm} \sum_{j=1}^{3} n_F[E_j^s(k)] - 1/2. \tag{14}$$

Note that this equation determines M_z in a self-consistent way because the energy spectra [Eq. (9)] on the left-hand side of Eq. (14) depend on M_z. $n_F(x) = 1/(1+e^{\beta x})$ is the Fermi-Dirac factor.

C. Mean-field equations for the state with $Q = Q'$: State II

Now, if we impose to the bond parameters Q and Q' to be equal, the free energy per site will become

$$f_{\mathrm{II}}(T,h) = \frac{1}{3}(3JQ^2 + 2J_\perp P^2) - \frac{1}{3}(3J + 2J_\perp)M_z(M_z+1) + \frac{h}{2} - \frac{k_B T}{2N_t}\sum_k \sum_{s=\pm} \sum_{j=1}^{3} \ln[1 + e^{-\beta E_j^s(k)}], \tag{15}$$

and the energy spectra reduce to

$$E_1^{\pm}(k) = -h' \pm J_1 \sin k,$$

$$E_2^{\pm}(k) = \frac{1}{2}[-h' - h'' \pm \epsilon_-(k)],$$

$$E_3^{\pm}(k) = \frac{1}{2}[-h' - h'' \pm \epsilon_+(k)], \tag{16}$$

with $\epsilon_{\pm}(k)$ becoming,

$$\epsilon_{\pm}(k) = \sqrt{[2J_1 \sin k \pm J_\perp M_z]^2 + 2J_{\perp 1}^2}.$$

The mean-field equations in this case with $Q' = Q$ are

$$Q = \frac{-1}{4JN_t}\sum_k \sum_{s=\pm} \sum_{j=1}^{3} \frac{\partial E_j^s(k)}{\partial Q} n_F[E_j^s(k)],$$

$$P = \frac{-1}{8J_\perp N}\sum_k \sum_{s=\pm} \sum_{j=2}^{3} \frac{\partial E_j^s(k)}{\partial P} n_F[E_j^s(k)], \tag{17}$$

with

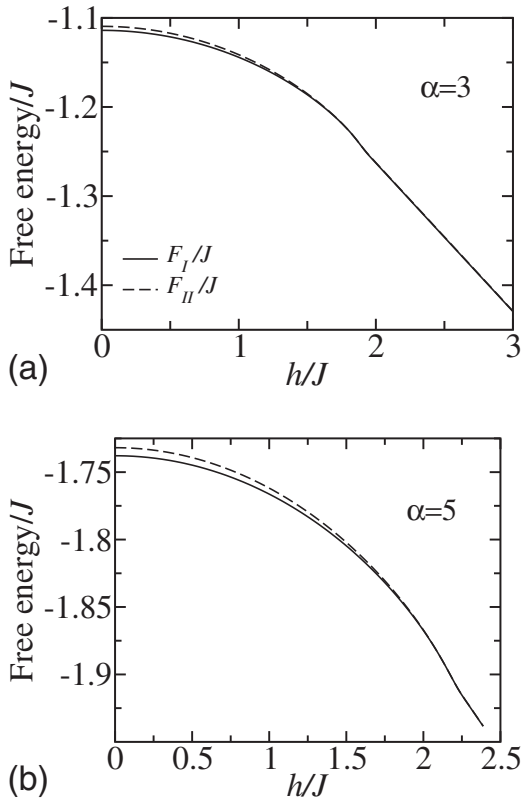

FIG. 2. The free energies f_{I} and f_{II} calculated at $T=0.01J$ are plotted as functions of field h for (a) $\alpha=3$ and (b) $\alpha=5$. The state with $Q\neq Q'$ is the stable one for all fields.

$$\frac{\partial E_1^s}{\partial Q} = 2sJ \sin k,$$

$$\frac{\partial E_2^s}{\partial Q} = 2s\frac{J \sin k}{\epsilon_-(k)}(2J_1 \sin k - J_\perp M_z),$$

$$\frac{\partial E_3^s}{\partial Q} = 2s\frac{J \sin k}{\epsilon_+(k)}(2J_1 \sin k + J_\perp M_z),$$

$$\frac{\partial E_2^s}{\partial P} = \frac{2sJ_\perp J_{\perp 1}}{\epsilon_-(k)},$$

$$\frac{\partial E_3^s}{\partial P} = \frac{2sJ_\perp J_{\perp 1}}{\epsilon_+(k)}. \tag{18}$$

The expression for the magnetization remains the same as in Eq. (14), with the energy spectra replaced by those in Eq. (16).

D. Comparison of the free energies of the states I and II

We report in Figs. 2(a) and 2(b) the free energies, f_{I} and f_{II}, for two rung coupling values ($\alpha=3$ and 5) as functions of magnetic field. The thermodynamically stable state is always state I with $Q\neq Q'$. Also, we found that a field-induced phase transition does not exist because no crossing between the free energies takes place. Note however that the difference between these free energies becomes negligibly small when the field becomes large ($h>J$) with the free energy for state I being the lowest always. In the strong-field limit where all the bond parameters vanish, the free energies f_{I} and f_{II} become equal. In the remainder of this paper, only state I will be used except in Sec. VII where an analytic solution is found for the simpler case of state II.

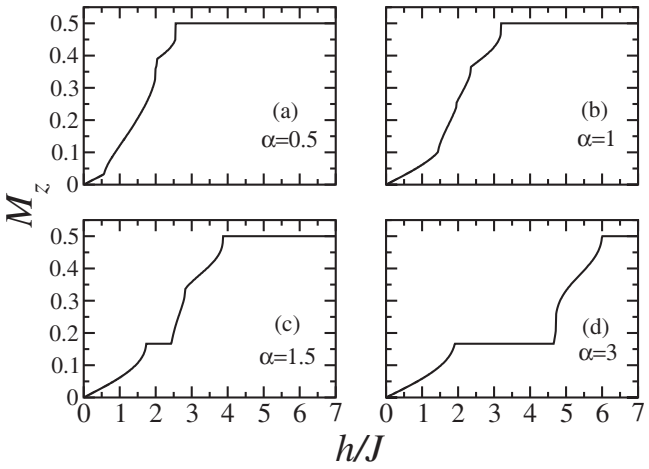

FIG. 3. The magnetization M_z is drawn as a function of magnetic field for four values of α; (a) $\alpha=0.5$, (b) $\alpha=1$, (c) $\alpha=1.5$, and (d) $\alpha=3$.

III. FIELD DEPENDENCE OF MAGNETIZATION AND SUSCEPTIBILITY

The quantity we can readily compare to existing exact numerical data for the Heisenberg three-leg ladder is the magnetization. Thus we start by analyzing its field dependence for several values of the rung coupling. We found that there are two distinct regimes in this field dependence; one in which the magnetization is characterized by two plateaus in the strong rung coupling limit and one in which the magnetization is characterized by only one plateau in the weak rung coupling regime. There exists a threshold value for the rung coupling, α_0, below which only the saturation plateau shows up in the magnetization and above which an additional plateau occurs at one third of the saturation magnetization. We will analyze the reason for the existence of these two behaviors and calculate the $(\alpha, h/J)$ phase diagram.

Figures 3(a)–3(d) show the magnetization as a function of field for four values of α. While a plateau at the third of the saturation magnetization $M_s/3$ occurs for $\alpha=1.5$ or 3, none takes place for $\alpha=0.5$ and 1. The plateau at $M_s/3$ for $\alpha=3$ is wider than for $\alpha=1.5$. The magnetization versus field for $\alpha=3$ is in good agreement with the result in Ref. 6. Figure 4 shows the magnetization and susceptibility χ for $\alpha=3$. χ is characterized by three sharp peaks at very low temperature and is zero for the fields corresponding to the plateaus. The field dependence of χ is also in good qualitative agreement with the result of Ref. 6. It is now important to find the field dependent value of α, above which a plateau at $M_s/3$ sets in. Note that the saturation magnetization $M_s=1/2$ can be real-

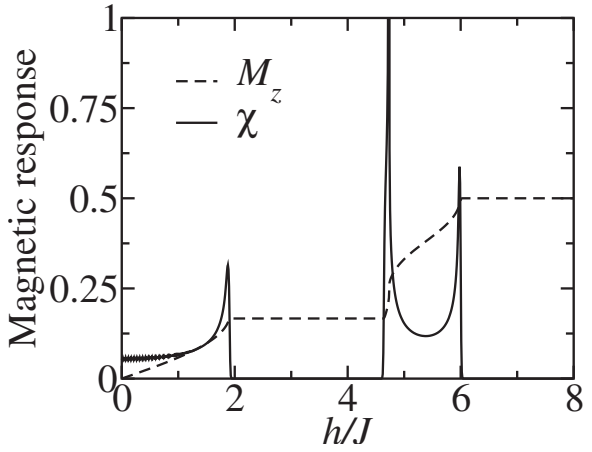

FIG. 4. The magnetization M_z and the spin susceptibility χ are drawn as functions of magnetic field for $\alpha=3$ and $T=0.005J$.

ized for any coupling α when the field exceeds the upper critical field h_{c2}. The latter is found to increase practically linearly with α. The field, above which the intermediate plateau at $M_s/3$ appears, is known as the lower critical field h_{c1}. The latter also increases linearly with α but with a slope much smaller than for h_{c2}.

Figure 5 displays the zero-temperature $(\alpha, h/J)$ phase diagram. The latter consists of five regimes, which are distinguished by the way the magnetization behaves as a function of field. These regimes are (i) the one where the magnetization assumes the maximum value $M_z \equiv M_s = 1/2$, forming a plateau in the strong-field domain for any rung coupling α. (ii) The regime with the plateau at one third of the saturation magnetization, $M_z = M_s/3$, is realized for $h_{c1} < h < h_+$ and $\alpha > \alpha_0$, with $\alpha_0 \approx 1.01$ and h_+ the field above which the magnetization departs from the $M_z = M_s/3$ plateau. (iii) The region with magnetization $M_z < M_s/3$ is realized in the weak-field limit for $\alpha > \alpha_0$. (iv) The region with no intermediate plateau at $M_s/3$ is realized for fields smaller than h_{c2} and for

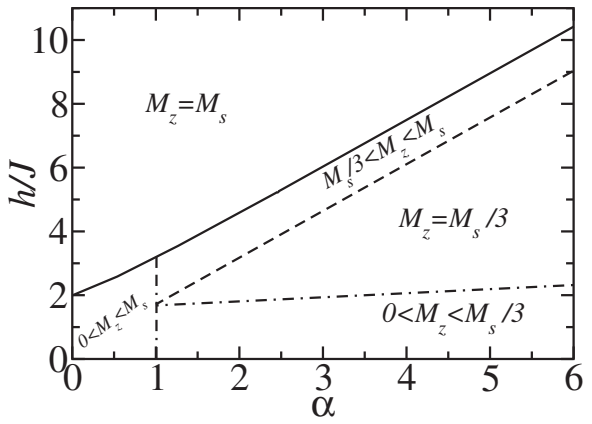

FIG. 5. The $(\alpha, h/J)$ phase diagram for the three-leg ladder is displayed. The critical fields h_{c1} and h_{c2} are displayed as continuous and dashed-dotted lines, respectively. M_s stands for the saturation value of the magnetization. For $\alpha < \alpha_0$, the plateau at $M_s/3$ does not exist $(\alpha_0 \approx 1.01)$. This phase diagram agrees qualitatively well with the one calculated by Cabra *et al.* (Ref. 7) in the large rung coupling and field regime.

$\alpha < \alpha_0$. (v) Finally, the region with the magnetization between $M_s/3$ and M_s is realized for $\alpha > \alpha_0$ and fields $h_+ < h < h_{c2}$. The most interesting in this phase diagram is that the $M_s/3$ plateau does not extend to weak rung couplings. The present mean-field approach indicates that $\alpha > \alpha_0 \approx 1.01$ is a necessary condition for the appearance of the plateau at $M_s/3$ in the magnetization. The lower (h_{c1}) and upper (h_{c2}) critical fields are shown in Fig. 5 as a dashed-dotted line and a continuous line, respectively. The field h_+, above which the magnetization departs from the $M_s/3$ plateau, is shown as a dashed line that satisfies $h_+(\alpha) \approx 1.46\alpha J$. h_{c1} and h_{c2} are approximately given by

$$h_{c1} \approx 1.53J + 0.13J\alpha,$$

$$h_{c2} \approx 2J + 1.46J\alpha. \tag{19}$$

The fits in Eq. (19) give $h_{c1} \approx 1.92J$ (very close to the actual value $1.91J$) for $\alpha=3$, which is in excellent agreement with the numerical result of Tandon *et al.*[6] However, the width of the $M_s/3$ plateau we find here $(2.79J)$ is greater than the one found by these authors, which is $1.88J$. This means that our value for h_+ does not compare well with Tandon *et al.* Note that the upper critical field $h_{c2} \approx 6J$ [$6.38J$ using the fit in Eq. (19)] compares relatively well with theirs, which is about $6.5J$. In the limit $\alpha \to 0$, h_{c1} does not exist and h_{c2} tends to $2J$, which is the critical field for the single Heisenberg chain.[2,11]

IV. FIELD DEPENDENCE OF THE SPIN BOND PARAMETERS

Figures 6(a) and 6(b) show the field dependence of the mean-field parameters for $\alpha=3$ and 1, respectively. The temperature is $(0.005J)$ practically zero for both coupling values. We see that the bond parameters show plateaus for $\alpha=3$ but no plateaus occur for $\alpha=1$. We checked that a plateau appears in the spin bond parameters only above the threshold value α_0. When the field is greater than h_{c2}, all the bond parameters are zero. Next we discuss separately the regimes below and above α_0.

A. Strong rung coupling regime $\alpha \gtrsim \alpha_0$

This is the regime where the $M_s/3$ intermediate plateau appears in the magnetization. In this regime, the spin bond parameters are all characterized by a plateau in the same field region where the $M_s/3$ magnetization plateau occurs. The three bond parameters Q, Q', and P do not show the same field dependence in general. For example, for $\alpha=3$, Q decreases when the field h increases away from zero, levels off for all the fields $h_{c1} < h < h_+$ corresponding to the $M_s/3$ plateau, starts to vary again when the field exceeds h_+, becomes even negative, and passes through a minimum before vanishing at h_{c2}. Q' is smaller than Q but shows the same field dependence as Q for the fields $h < h_+$. Q' increases sharply for $h > h_+$, passes through a maximum, and then vanishes at h_{c2}. The fact that Q becomes negative but not Q' is an indication that the spin bond *topology* along the rungs $\ldots(\uparrow_{i,1}\downarrow_{i,2})(\downarrow_{i,2}\uparrow_{i,3})\ldots$ becomes frustrated and that the phase

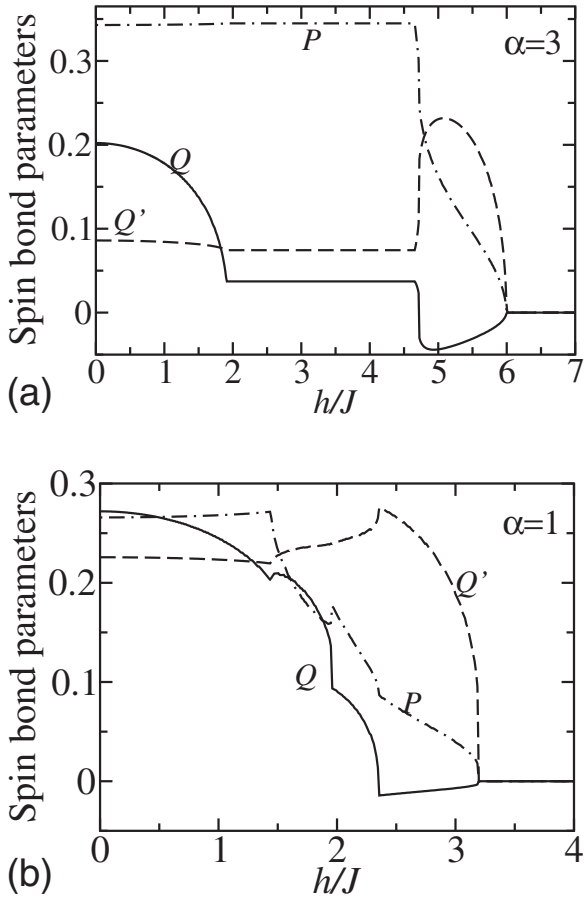

FIG. 6. The mean-field parameters are plotted as functions of magnetic field for two values of α: (a) $\alpha=3$ and (b) $\alpha=1$. Temperature is $T=0.005J$.

per plaquette becomes irrelevant because the magnetic field tends to align all the spins in its direction. $(\uparrow_{i,1}\downarrow_{i,2})$ designates a spin singlet arrangement. This explanation is supported by the fact that in the field region where Q becomes negative the rung bond parameter P decreases sharply. Contrary to Q and Q', the parameter P increases with field when $h<h_{c1}$, forms a plateau for $h_{c1}<h<h_{+}$, then decreases, and finally vanishes at h_{c2}. It is worth to mention that the phase transitions occurring as a consequence of the sudden changes in the bond parameters happen at the same fields where the magnetization shows its abrupt changes.

Near the critical points of the parameters Q, Q', and P, here for $\alpha=3$ and for any $\alpha>\alpha_0$, one can expand the ground-state energy and get analytical expressions for these parameters (refer to Sec. VII where this is done for the simpler case of state II).

B. Weak rung coupling regime $\alpha \lesssim \alpha_0$

Contrary to the case $\alpha>\alpha_0$, the parameters Q, Q', and P show no plateau in the weak-coupling limit $\alpha<\alpha_0$. Similarly magnetization shows no intermediate plateau in this case. Figure 6(b) displays the bond parameters versus field for $\alpha=1$. These parameters are now characterized by cusps, which are due to the crossing of the energy bands by the chemical potential (field h) of the JW fermions as the field varies. To understand why in the strong-coupling regime plateaus exist but not in the weak-coupling regime, we will analyze in the next section (Sec. V) the field dependence of the energy band structure.

V. INTERPRETATION OF THE PLATEAUS IN MAGNETIZATION AND BOND PARAMETERS

In order to understand why the $M_s/3$ plateau exists for $\alpha>\alpha_0$ but not for $\alpha<\alpha_0$, we calculate the energy spectra as functions of the wave number k for different values of the rung coupling and magnetic field. In this way we also explain the existence of the threshold value of the rung coupling α_0. We consider first a value for α larger than α_0; $\alpha=3$. Figures 7(a)–7(d) display the spectra for the fields $h=0$, J, $3J$, and $6J$, respectively. In terms of the JW fermions, the magnetic field acts as their chemical potential so that when the field (Zeeman energy $h=g\mu_B B$) is varied within the gap between the two upper-energy bands and the ones just beneath them, no change occurs in M_z, Q, Q', or P. This leads to a plateau in each of these quantities. This is well illustrated for $h=3J$ in Fig. 7(c). When the field goes above the upper-energy bands, the saturation regime of magnetization is entered and all bond parameters vanish.

When $\alpha<\alpha_0$, the gap between the upper-energy and intermediate-energy bands closes. For $\alpha=0$ and zero field, the three chains of the ladder are completely decoupled. The excitation energy spectra in this case are threefold degenerate and are equivalent to the des Cloizeaux spectrum; namely, $E(k)=J(1+2Q)|\sin k|$.[17] Note that the excitation energies are obtained by considering the energies that are above the chemical potential h. When the rung coupling α increases, this degeneracy is progressively lifted. The excitation spectra consist then of three distinct bands as Eqs. (9) indicate. One band remains gapless but the other two become gapped as Fig. 8(a) shows for $\alpha=1$ and zero field ($h=0$). For as long as a gap does not exist between the upper-energy bands and the two ones just beneath them, no plateau shows up in the magnetization or the mean-field parameters. Figure 8(b) shows the spectra for $\alpha=1$ and $h=J$ where no gap exists between the upper-energy and intermediate-energy bands. In the weak rung coupling regime $\alpha<\alpha_0$, when the field increases, the chemical potential h goes from crossing only the intermediate-energy bands to crossing the latter and the upper-energy ones together, and then to crossing the latter alone. Finally, in the strong-field limit (with $h>h_{c2}$), all bands fall below the chemical potential implying that any variation in field ($h>h_{c2}$) affects neither magnetization nor spin bond parameters.

To illustrate even better the existence of the threshold value $\alpha_0\approx 1.01$, we plot the energy spectra for a α slightly greater than α_0; that is $\alpha=1.1$, and for $h=1.75J$ in Fig. 9. One can note that a very small gap has opened near zero energy, which is the JW Fermi energy indicated by the horizontal dashed line in this figure. The present analysis based on the lifting of degeneracy and based on the opening of a gap between bands makes it clear that the value of the rung coupling, above which magnetization displays a plateau, must be greater than zero.

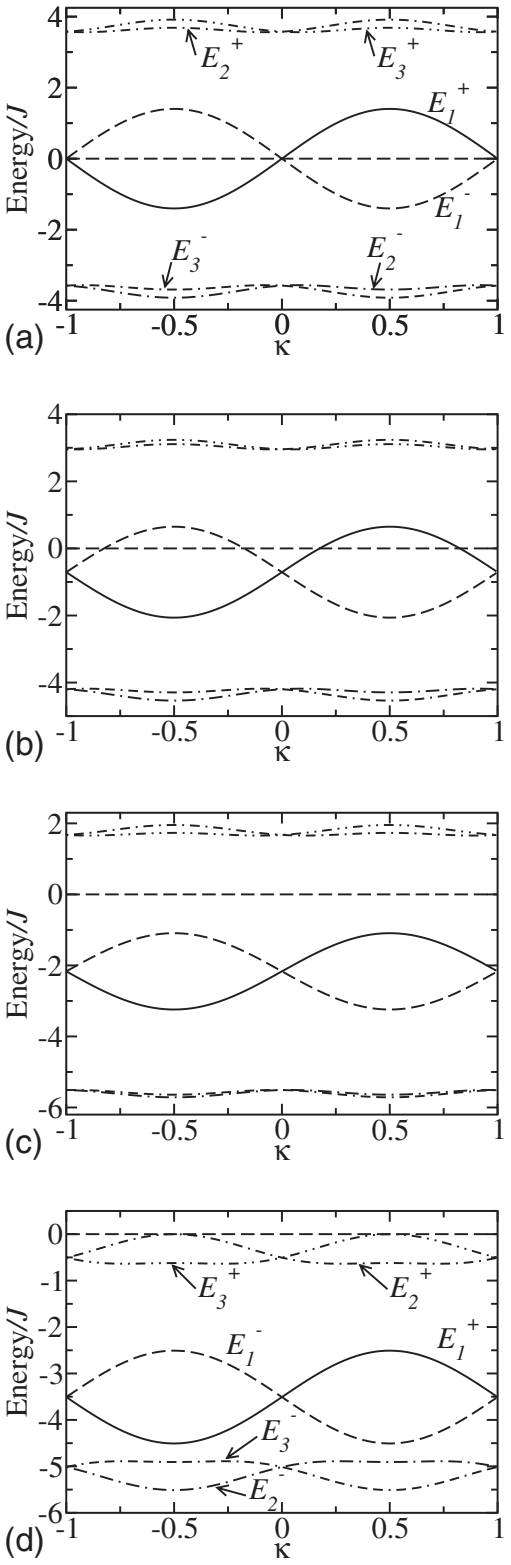

FIG. 7. The energy spectra for the three-leg ladder are drawn as functions of $\kappa=k/\pi$. The magnetic field is $h=0$ in (a), $h=J$ in (b), $h=3J$ in (c), and $h=6J$ in (d). Temperature is $T=0.005J$ (practically zero), and $\alpha=3$. The continuous line is E_1^+, the dashed line is E_1^-, the dashed-dotted line is E_2^+, the dashed-dotted-dotted line is E_3^+, the dashed-dashed-dotted line is E_3^-, and the long-dashed-dotted line is E_2^-. The horizontal dashed line designates the position of the Fermi energy for the JW fermions.

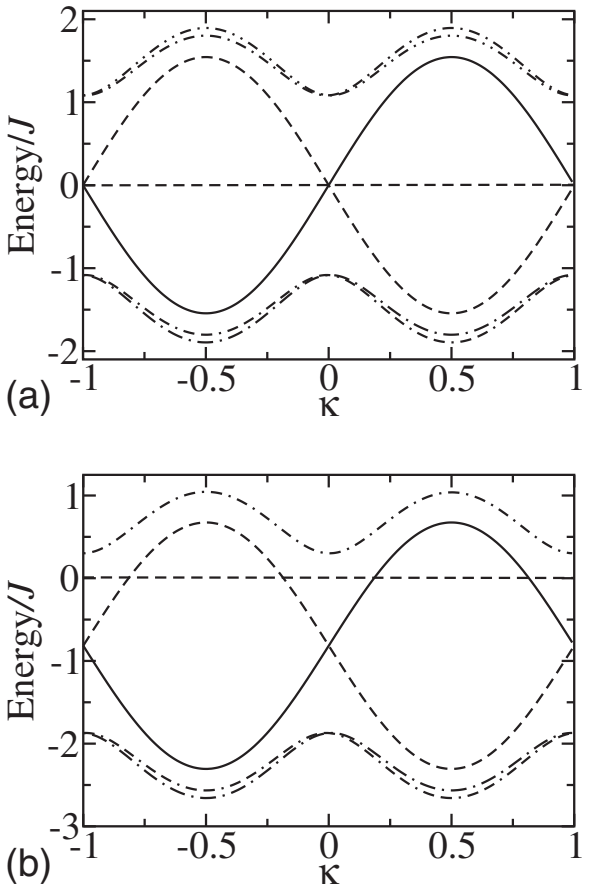

FIG. 8. The energy spectra are drawn as functions of $\kappa=k/\pi$ for magnetic fields $h=0$ in (a) and $h=J$ in (b). Temperature is zero and $\alpha=1$. The continuous line is E_1^+, the dashed line is E_1^-, the dashed-dotted line is E_2^+, the dashed-dotted-dotted line is E_3^+, the dashed-dashed-dotted line is E_3^-, and the long-dashed-dotted line is E_2^-. Note that in (b) E_2^+ and E_3^+ are practically equal. So we chose to draw only E_2^+. The horizontal dashed line designates the position of the Fermi energy for the JW fermions. Notice that a gap does not exist between the upper-energy bands, E_2^+ and E_3^+, on one hand and $E_1^\pm$ on the other hand for $\alpha=1$.

VI. EFFECT OF TEMPERATURE ON QUANTUM CRITICALITY

Figure 10 shows the magnetization $M_z(h,T)$ versus field for six values of temperature T and for $\alpha=3$. The strongest temperature dependence is shown by the $M_s/3$ plateau, which disappears completely when T becomes greater than about $0.4J$. The fading away of the plateau is caused by the filling of the gap in E_2^+ and E_3^+ by thermally excited JW fermions, i.e., by the filling of the gap by thermal induced spin excitations. Figure 11 displays the spin susceptibility $\chi(h,T)=\partial M_z/\partial h$ as a function of the field for the same value of α and for the same six temperatures as in Fig. 10. At very low temperatures, $\chi(h,T)$ is characterized by three peaks. However as temperature increases, the peaks decrease in amplitude and completely disappear again for $T\geq 0.4J$. The susceptibility, which is zero between the first peak and the second one at zero T, becomes nonzero at finite T (a consequence of the disappearance of the intermediate mag-

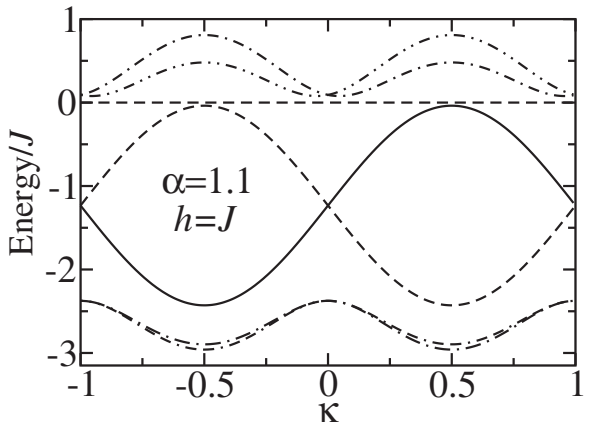

FIG. 9. The energy spectra are drawn as functions of $\kappa=k/\pi$ for magnetic fields $h=1.75J$, zero temperature, and $\alpha=1.1$. See Fig. 7 for legend. Notice that a gap between the upper-energy bands E_2^+ and E_3^+, and the bands E_1^+ and E_1^- develops, which means that a plateau appears in the magnetization and the mean-field parameters.

netization plateau at $M_s/3$ due to the appearance of spin excitations in the gap).

The effect of temperature on the spin bond parameters is reported in Fig. 12(a) for $\alpha=3$ and $T=0.1J$, and in Fig. 12(b) for $\alpha=3$ and $T=0.5J$. We found that the critical behavior in the bond parameters disappears as soon as temperature becomes nonzero, yielding only a crossover behavior. The plateaus also tend to disappear when temperature increases as clearly illustrated for $T=0.5J$ in Fig. 12(b) where the plateau in Q has completely disappeared. This behavior (the replacement of criticality with a crossover when temperature becomes nonzero) is similar to that found previously in the Heisenberg chain and two-leg ladder.[2]

VII. ANALYTICAL SOLUTION FOR THE BOND PARAMETERS IN STATE II

A. Zero field

To illustrate analytically the existence of the quantum phase transitions, we consider for simplicity state II with $Q=Q'$, first in zero field, and expand the ground-state energy in powers of $1/\alpha$ in the limit α large. The ground-state energy can be calculated using the zero-T limit in Eq. (15). At zero temperature, only the energy bands below the Fermi energy of the JW fermions contribute to the integrals in Eq. (15). One gets the ground-state energy,

$$E_{\mathrm{GS}}=\frac{1}{3}(3JQ^2+2J_\perp P^2)-\frac{1}{3}\int_0^\pi \frac{dk}{2\pi}E_1(k)-\frac{1}{3}\int_0^\pi \frac{dk}{2\pi}\epsilon(k), \tag{20}$$

with

$$E_1(k)=J_1\sin k,$$

$$\epsilon(k)=\sqrt{4J_1^2\sin^2 k+2J_{\perp 1}^2}. \tag{21}$$

In the limit $\alpha\gg 1$, $\epsilon(k)$ can be expanded in even powers of $1/\alpha$ as

$$\epsilon(k)=\sqrt{2}J_{\perp 1}\left[1+\frac{J_1^2}{J_{\perp 1}^2}\sin^2 k-\frac{J_1^4}{J_{\perp 1}^4}\sin^4 k\right]+\mathcal{O}(\alpha^{-6}),$$

because $\frac{J_1}{J_{\perp 1}}=\frac{1}{\alpha}\frac{1+2Q}{1+2P}$. We replace P by its mean-field value and we focus only on the parameter Q for the sake of simplicity. We write the ground-state energy as a series in powers of $J_1=J(1+2Q)$ after performing the integrals over k. The result is

$$E_{\mathrm{GS}}=E_0+\left(a_1-\frac{1}{2}\right)J_1+\left(a_2+\frac{1}{4J}\right)J_1^2+a_4J_1^4+\ldots \tag{22}$$

Here E_0 is a J_1-independent term, and the coefficients are analytically given by

$$a_1=-\frac{1}{3}\int_0^\pi \frac{dk}{2\pi}\sin k=-\frac{1}{3\pi},$$

$$a_2=-\frac{2\sqrt{2}}{6J_{\perp 1}}\int_0^\pi \frac{dk}{2\pi}\sin^2 k=-\frac{\sqrt{2}}{12J_{\perp 1}},$$

$$a_4=\frac{2\sqrt{2}}{6J_{\perp 1}^3}\int_0^\pi \frac{dk}{2\pi}\sin^4 k=\frac{\sqrt{2}}{16J_{\perp 1}^3}. \tag{23}$$

Minimizing E_{GS} with respect to J_1, $\partial E_{\mathrm{GS}}/\partial J_1=0$ leads to $Q\approx 1/3\pi$ in the limit $\alpha\to\infty$, in excellent agreement with the result obtained numerically from Eq. (17).

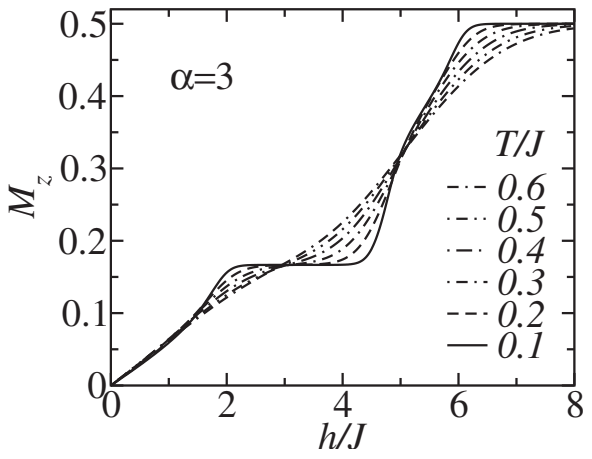

FIG. 10. The magnetization M_z is plotted versus field for $\alpha=3$ and for several values of temperature.

B. Nonzero field

An expansion is possible for the ground-state energy even in the presence of the external magnetic field. For simplicity, we consider fields in the vicinity of h_{c1} and we assume that α is large enough for a gap to appear in the energy spectra, i.e., for a magnetization plateau to appear at $M_s/3$. The ground-state energy is given by

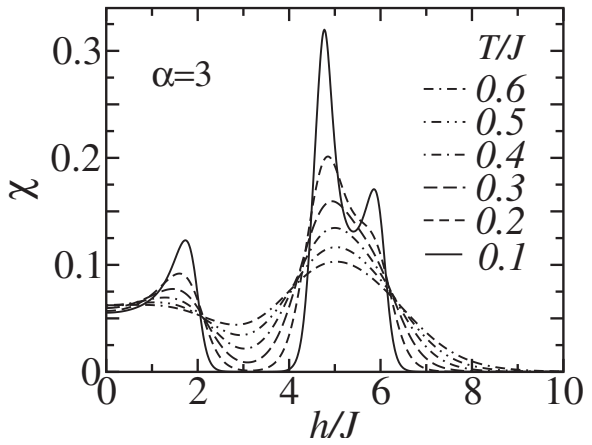

FIG. 11. The magnetic susceptibility χ along the z axis is plotted as a function of the magnetic field h.

$$E_{\mathrm{GS}} = JQ^2 + \frac{2}{3}J_\perp P^2 - \left(J + \frac{2}{3}J_\perp\right)M_z(M_z+1) + \frac{h}{2} - \frac{1}{6}\int' \frac{dk}{2\pi}[E_1^-(k) + E_1^+(k)] - \frac{1}{6}\int' \frac{dk}{2\pi}[\epsilon^-(k) + \epsilon^+(k)], \tag{24}$$

where the interval of integration ($\int'$) consists of only those k points, for which the energies are negative at zero temperature. In the limit α large, because $\epsilon_+(k)+\epsilon_-(k)$ is an even function in J_1, the expansion in powers of $J_1/\mathcal{J}_\perp$ contains only even powers. Up to the fourth order, one gets

$$\epsilon_+ + \epsilon_- \approx \mathcal{J}_\perp\left\{1 + \frac{2J_1^2\sin^2 k}{\mathcal{J}_\perp^2}\left[1 - \frac{2J_\perp^2 M_z^2}{\mathcal{J}_\perp^2}\right] - \frac{4J_1^4\sin^4 k}{\mathcal{J}_\perp^4}\left[1 + 36\frac{J_\perp^2 M_z^2}{\mathcal{J}_\perp^2}\right]\right\}, \tag{25}$$

with $\mathcal{J}_\perp^2 = 2J_{\perp 1}^2 + J_\perp^2 M_z^2$. This yields

$$E_{\mathrm{GS}}(h) = E_0(h) + \left[a_1(h) - \frac{1}{2}\right]J_1 + \left[a_2(h) + \frac{1}{4J}\right]J_1^2 + a_4(h)J_1^4 + \ldots \tag{26}$$

where the coefficients are now field dependent. The magnetic field is known to shift the chemical potential of the JW fermions. This changes the bounds of the intervals of integration involved in the expressions of these coefficients. For example, the magnetization reaches the 1/3 plateau when the field is such that both bands $E_1^\pm(k)$ go completely below the Fermi energy. For $h_{c1} \lesssim h \ll h_+$, the chemical potential is between the upper-energy bands, E_2^+ and E_3^+, and the medium-energy ones, $E_1^\pm$ (as illustrated in Fig. 7(c) for $\alpha=3$). In such a situation, the coefficients assume the following expressions:

$$a_1 = 0,$$

$$a_2 = -\frac{1}{6}\frac{1}{\mathcal{J}_\perp}\left[1 - \frac{2J_\perp^2 M_z^2}{\mathcal{J}_\perp^2}\right],$$

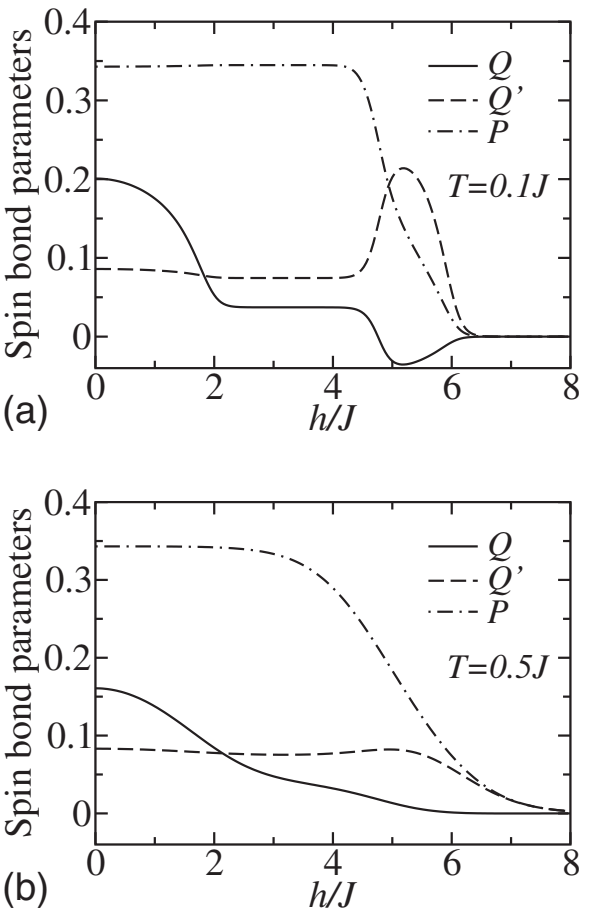

FIG. 12. The spin bond parameters are drawn as functions of field for rung coupling $\alpha=3$ and temperatures $T=0.1J$ in (a) and $T=0.5J$ in (b).

$$a_4 = \frac{1}{4}\frac{1}{\mathcal{J}_\perp^3}\left[1 + 36\frac{J_\perp^2 M_z^2}{\mathcal{J}_\perp^2}\right]. \tag{27}$$

For fields $h_{c1} < h < h_+$ corresponding to the magnetization plateau at $M_z = M_s/3 = 1/6$, minimizing $E_{\mathrm{GS}}(h)$ in Eq. (26) with respect to J_1 gives

$$Q \equiv Q_p \approx \frac{1}{2\left(\frac{3}{2}\frac{\mathcal{J}_\perp}{J} - 1\right)}, \quad \alpha \gg 1, \tag{28}$$

in fairly good agreement with the numerically calculated values of Q using Eq. (17). For example, the value calculated using the approximation [Eq. (28)] is $Q_p \approx 0.051$ for $\alpha=3$, while the value obtained using Eq. (17) is 0.049. For $\alpha=10$, the values are respectively $Q_p \approx 0.014\,19$ and $0.014\,08$, hence implying a difference of less than a percent. Note that Q is not field dependent on the plateau, a result Eq. (28) satisfies exactly.

Following the same procedure as in Ref. 2, we find that for fields slightly below the lower critical field h_{c1}, the parameter Q assumes the expression,

$$Q = Q_p + c_1(h_{c1} - h)^{1/2}, \quad c_1 = \frac{\sqrt{2}}{3\pi\sqrt{J(1+2Q_p)}}. \quad (29)$$

Here, $h_{c1}=J(1+2Q_p)+J/3+J_\perp/6$. As for the magnetization, for h slightly smaller than h_{c1}, following again the same procedure as in Ref. 2, Eq. (14) gives

$$\frac{M_z}{M_p} = 1 - \frac{2\sqrt{2h_{c1}}}{\pi\sqrt{J(1+2Q_p)}}\left(1 - \frac{h}{h_{c1}}\right)^{1/2}, \quad h \lesssim h_{c1}, \quad (30)$$

where $M_p=M_s/3$. The spin susceptibility for $h \lesssim h_{c1}$ is

$$\chi = \frac{\partial M_z}{\partial h} = \frac{\sqrt{2}}{\pi\sqrt{J(1+2Q_p)h_{c1}}}\left(1 - \frac{h}{h_{c1}}\right)^{-1/2}, \quad (31)$$

hence indicating a divergence governed by the mean-field type exponent 1/2. In the plateau regime of the magnetization above h_{c1}, the susceptibility is zero. Thus the divergence is observed only below h_{c1}. Near the upper critical field h_{c2}, the magnetization and susceptibility are obtained by replacing h_{c1} by h_{c2}, Q_p by zero, and M_p by M_s in Eqs. (30) and (31).

VIII. CONCLUSIONS

The spin-$\frac{1}{2}$ antiferromagnetic three-leg Heisenberg ladder in the presence of an external magnetic field is studied. Upon treating this system within the bond mean-field theory, we find that it is characterized by zero-T spin bond order, which disappears when field reaches the upper critical field h_{c2}. The coupling field phase diagram is calculated. It is found that for the $\frac{M_s}{3}$-magnetization plateau to occur the rung coupling must exceed a threshold value. M_s is the saturation magnetization. Above this threshold coupling, each of the spin bond parameters is characterized by two zero-T critical points: one at the lower critical field h_{c1} and the second one at the upper critical field h_{c2}. The bond order is simply interpreted as the probability for adjacent spins to form a spin singletlike object. The magnetization and spin susceptibility versus field we calculated agree well with existing numerical data, a fact that indicates that the present approach works well. The effect of temperature on quantum criticality is studied. It is found that the criticality is replaced by a crossover regime once temperature becomes nonzero.

ACKNOWLEDGMENTS

This work was supported by the Natural Sciences and Engineering Research Council of Canada (NSERC) and the Laurentian University Research Fund (LURF).

[1] S. Sachdev, *Quantum Phase Transitions* (Cambridge University Press, New York, 1999).
[2] M. Azzouz, Phys. Rev. B **74**, 174422 (2006).
[3] M. Azzouz, Phys. Rev. B **48**, 6136 (1993).
[4] B. Frischmuth, B. Ammon, and M. Troyer, Phys. Rev. B **54**, R3714 (1996).
[5] M. Azzouz and K. A. Asante, Phys. Rev. B **72**, 094433 (2005).
[6] K. Tandon, S. Lal, S. K. Pati, S. Ramasesha, and D. Sen, Phys. Rev. B **59**, 396 (1999).
[7] D. C. Cabra, A. Honecker, and P. Pujol, Phys. Rev. Lett. **79**, 5126 (1997).
[8] D. C. Cabra, A. Honecker, and P. Pujol, Phys. Rev. B **58**, 6241 (1998).
[9] P. Jordan and E. Wigner, Z. Phys. **47**, 631 (1928).
[10] I. Affleck and J. B. Marston, Phys. Rev. B **37**, 3774 (1988).
[11] J. B. Parkinson and J. C. Bonner, Phys. Rev. B **32**, 4703 (1985).
[12] M. Azzouz, L. Chen, and S. Moukouri, Phys. Rev. B **50**, 6233 (1994).
[13] M. Azzouz and C. Bourbonnais, Phys. Rev. B **53**, 5090 (1996).
[14] M. Azzouz, B. Dumoulin, and A. Benyoussef, Phys. Rev. B **55**, R11957 (1997).
[15] M. Azzouz, K. Shahin, and G. Y. Chitov, Phys. Rev. B **76**, 132410 (2007).
[16] J. R. Schrieffer, *Theory of Superconductivity* (Benjamin, New York, 1964).
[17] J. des Cloizeaux and J. J. Pearson, Phys. Rev. **128**, 2131 (1962).